Fracture characterization for constraining reservoir characterization using AVOA: A case study from the Rulison field

Asghar Shams* and Colin MacBeth, Heriot-Watt Institute of Petroleum Engineering, Edinburgh, UK

This paper was prepared for presentation at the 8th International Congress of The Brazilian Geophysical Society held in Rio de Janeiro, Brazil, 14-18 September 2003.

Abstract

In order to build a more accurate reservoir model in a fractured media, a new technique is developed for anisotropy detection using 3D P-wave data on a fractured gas reservoir in Rulison field, Piceance basin, Colorado. This helps us improve our understanding of interaction between fractures and fluid flow behavior. Methodology includes robust restricted azimuth and offset pre-stack processing algorithm to preserve amplitude and anisotropy and then followed by a new analysis technique based on polarization filtering to preferentially separate the anisotropy from the geology response. Maps of magnitude and direction of anisotropy over horizon slices picked are produced for the target and a control horizon. Results demonstrate clear relationship between anisotropy anomalies and major faults as well as coherency attributes. There is also an obvious correlation between the anomalies and the expected ultimate recovery (EUR) map which can support fracture porosity model for reservoir simulation.

Introduction

In low matrix porosity and low permeability reservoirs, fractures control fluid flow and production rate. Permeability in fractured media is tied to two major factors which can control reservoir fluid behavior, (1) aperture and (2) fracture porosity (ϕ_F) (MacBeth, and Pickup, 2002 and Brown, et al., 2001). Therefore mapping fractures becomes a more crucial issue for reservoir simulation. Well logs such as FMS and FMI can be used to determine fracture orientation, but only with certain assumptions; moreover the predictions are limited to just around the wells. Because of wider spatial coverage of surface seismic data, fracture estimation from seismic becomes more important.

PP AVOA is starting to be regularly used as part of conventional interpretation methodology for fracture characterization. The effect of aligned vertical fractures on P-wave reflectivity is a function of incidence angle and azimuth which can be summarized as:

$$R_{pp}(\theta,\phi) = A + [B + D\cos 2(\phi)]\sin^2\theta + [C + E\cos 2(\phi) + F\cos 4(\phi)]\sin^2\theta\tan^2\theta$$

Where A, B, C, D, E, F are functions of the contrast and azimuthal anisotropy parameters across the reflection interface.

Re-writing the far-offset angle stack parallel (S_{par}) and perpendicular (S_{perp}) to some defined the principal direction gives:

$$S_{par} = G + A_{par} + N_1,\ S_{perp} = G + A_{perp} + N_2;$$

Where A_{par}, A_{perp} are the anisotropy contributions as defined above, G the geology, and N is noise (Shams, and MacBeth, 2002, 2003). Using this formulation we develop a new robust controlled procedure to isolate anisotropy anomalies for both parallel and perpendicular sectors. To further verify the results, polarization filtering is used to calculate and isolate geology from original parallel and perpendicular sectors. The geology is then filtered out from the original data to extract anisotropy attributes with similar conclusion.
Anisotropy anomalies are interpreted to fracture models which are in a good link to EUR.

Rulison Field

The target is a gas sand reservoir lies in Piceance basin, Colorado and encompasses approximately 12 squares miles (Figure 1). A small northwest plunging anticline nose is located in the southeastern portion of the field, and most probably has influenced fracturing found in Rulison. Gas is trapped in structurally enhanced stratigraphic traps, and natural fractures contribute to high

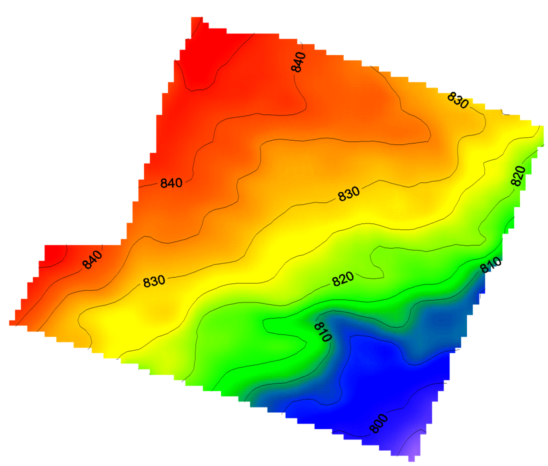

Figure 1: Structure map of a gas producer interval of Mesaverde interval in the Rulison field.

gas production rates from some part of reservoir. The productive interval is at the gas-saturated Mesaverde with extremely low matrix porosity and matrix permeability, the commercial production is controlled by natural fractures.
Based on new seismic interpretation there are two different sets of incoherency. Major faulting on Cameo Coal base of the zone of interest lies along the N30W. Coherency cube analysis shows the majority of Mesaverde gas production intervals are influenced by a trend along N50/60E which gradually change to N30W towards target base.

Dataset and Pre-stack processing flow

Seismic 3D data were acquired by Western Geophysical during April 1996. A total of 921 receiver locations were recorded for each source point. The receiver lines were 660 feet apart while the group spacing was 220 feet. The source interval was also 220 feet with a source line spacing of 1100 feet. This produced 110 foot * 110 foot cell size and a nominal fold of 40. Given the fixed spread geometry the fold pattern was pyramidal in shape with a very high fold in the center due to the extremely long offsets.

Rulison seismic acquisition pattern provides the wide azimuth and offset coverage necessary for *AVOA* studies and true *3D* imaging. However this particular acquisition geometry creates a patchy distribution of offset and azimuth that prevents straightforward analysis. Due to this condition we choose to follow the restricted-azimuth approach (Lynn et al. 1999) in order to boost the fold at each offset for each single CMP. Thus, the data are sorted into two azimuth sectors centered on directions parallel and perpendicular to a prescribed principal direction, which in this case can be attributed to fractures or stress. To maximize our return, a pre-stack processing flow is constructed to focus on preservation of azimuthal anisotropy signature. The processing is achieved by developing a method for parallel pre-stack restricted azimuth and offset processing (PRAOP). The main steps of this processing approach are: 1) relative amplitude preservation; 2) surface consistent; 3) removal of acquisition artifacts (offset-azimuth balancing, source and receiver consistency, acquisition direction) and geometric phase balancing; 4) removal of processing artifacts (migration effects, multiples, dip effects, binning, velocity analysis direction), combined with amplitude and frequency balancing.

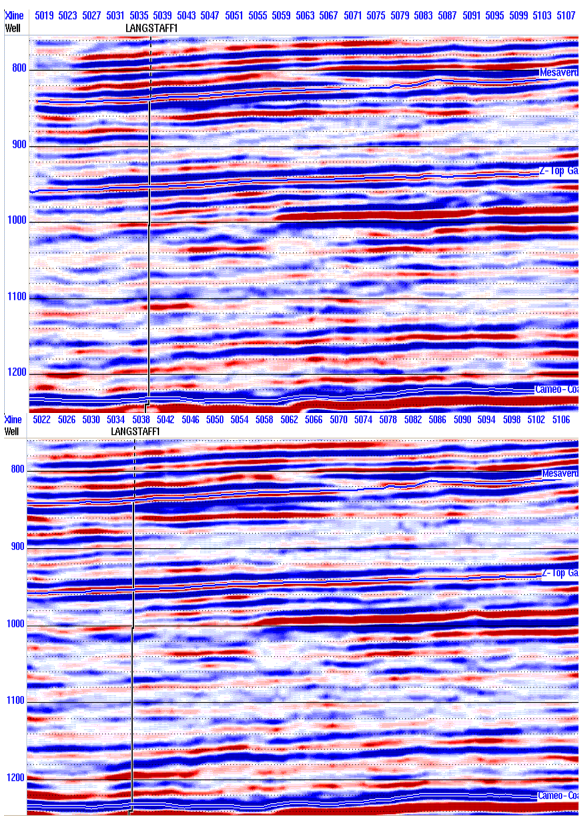

Figure 2: Time sections of PROAP processing results. Different sectors, top N60E and below N30W.

Basically we divide each dataset into two sectors parallel and perpendicular to the principal field direction in the Rulison field. This is based on previous studies (Lynn et al 1999) and also the original trend of several main faults; the estimated orientation is N30W. Each sector is defined by 55 degrees either side of N30W and N60E. The datasets are then moved through the processing, being treated individually but also simultaneously. Figure 2 shows two vertical sections, to illustrate the reduction in noise levels and artifacts achieved. After application of a post-stack amplitude and frequency balancing between the N30W sector and N60E sector, the anisotropy signature is revealed. To further verify the results, a different limited azimuth set (E-W and N-S) is also processed with similar conclusions.

Anisotropy enhancement

Two horizons slice picked through a gas producer interval of Mesaverde and Cameo-Coal have been taken to produce RMS amplitude maps for the 'fracture' parallel and perpendicular sectors. These two maps for each horizon are now further processed to extract the magnitude and orientation of the anisotropy signature. For each horizon two filter designed to separate either static and isotropic 'geological' response or anisotropy response in the presence of noise, on the concept of 3C polarization filtering (MacBeth, 2002). Having already balanced the data during processing, the idea behind the filter is that cross-plots of S_{par} versus S_{perp} lie on the line $S_{par} = S_{perp}$ if they are related to the geology signal, whilst the off-diagonal points are indicative of the anisotropy or the random noise. The polarization filter is designed to preferentially select either the geology or the anisotropy, and is applied as a template of spatially dependent weights to both RMS amplitude maps. Using either the isotropy filter or anisotropy filter magnitude of anisotropy can be calculated. To further verify result magnitude of anisotropy has been calculated using directly anisotropy filter and also using geology filter and then subtraction of geology from original data. The results showed consistency and quite similar maps with a more than 90% correlation coefficient. After separation, the magnitude and direction of the anisotropy can be computed according to projection geometry. For this the data needs to be cross-plotted, parallel against perpendicular, the intensity is defined by the distance between the ideal geology vector (1,1) and the actual result (u, v).

Variance attributes are generated to highlight faults and incoherent areas. The variance cube algorithm is a weighted moving variance. A cell of 3*3 inlines and crosslines with a 48 milliseconds time window is used as an operator for calculation. Figure 3 shows coherency maps of an interval of gas saturated Mesaverde (top) and also Came-coal (bottom) interval which is used as a control horizon. There are clearly high amplitudes incoherent patterns which are interpreted as faults and seismic visible fractures where incoherent (high amplitude) areas are displayed in high contrast.

Results

Figure 4 shows anisotropy maps of an interval of gas saturated Mesaverde (top) and came-coal horizon (bottom) and corresponding fault picks at the levels. A

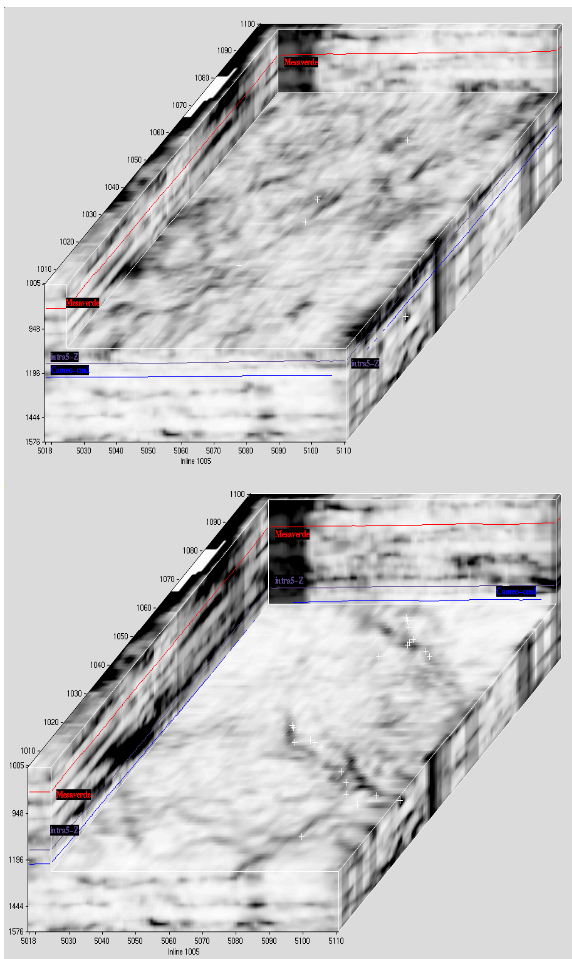

Figure 3: Coherency cubes of variance attributes analysis. Top is a gas producer interval Mesaverde, below is Cameo-Coal: the base of target zone. Faults and incoherent (high amplitude) areas are displayed in high contrast.

comparison of coherency maps with anisotropy shows a reasonable correlation between the trends in the AVOA anisotropy and faults determined from the coherency analysis. Thus the predicted anisotropy is an indicative of the fracturing within each fault compartment. In particular, the overall orientations and compartmentalization are very similar. The figures illustrate the large–scale faulting with a greater alignment of the fractures near the Northeast Southwest trending faults for Mesaverde and Northwest Southeast trending faults for Cameo-Coal.

Two high productive areas can be distinguished in Well EUR map (Figure 5). One is in the top of reservoir in southeastern portion of the field which is proportional to reservoir production model and the other one is located in the west part of the filed in the southwestern flank of the reservoir. It is a high permeable area with a high open fracture density. This portion is tied to high magnitude anisotropy map (figure 6). The best producer wells are located in the high intensity anisotropy anomalies. There is also a clear anisotropy direction from west to east through wells R40-20, RMV25-20 with negative and positive focal points of anisotropy around wells, CL-19, CL-7-21 (the best producers).

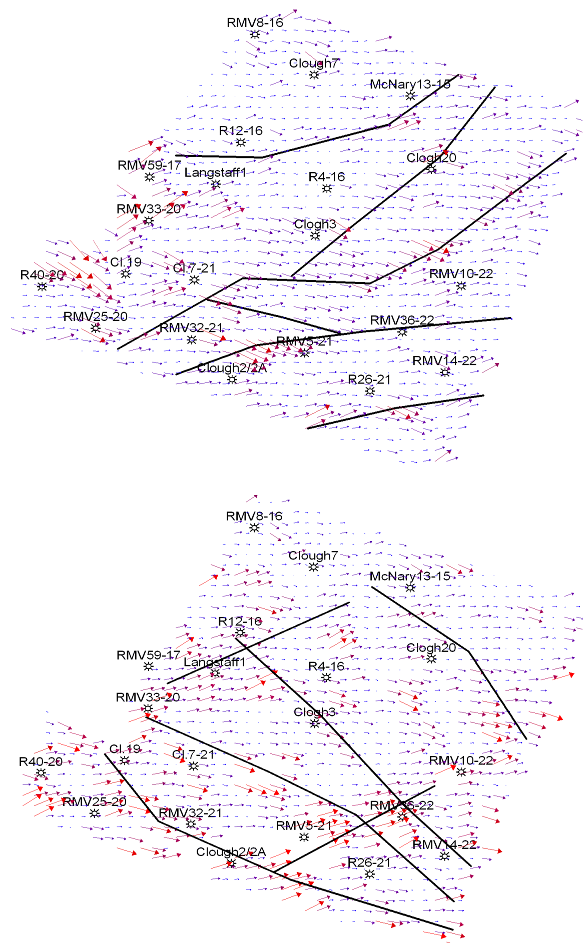

Figure 4: Two maps of seismic anisotropy results. Top is a gas producer interval Mesaverde, below is Cameo-Coal the base of target zone and corresponding interpreted faults.

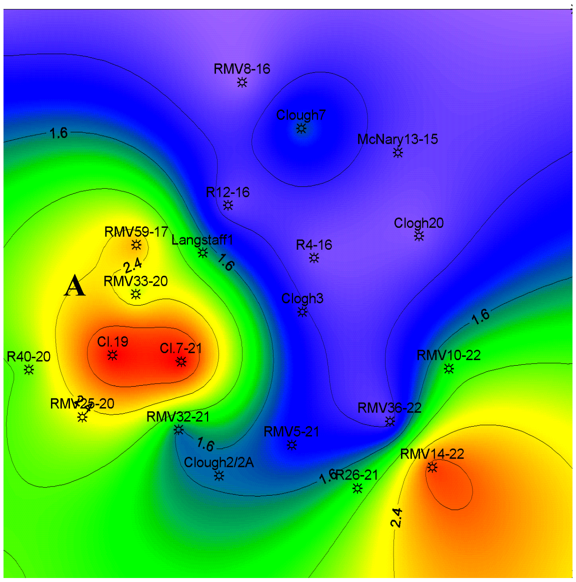

Figure 5: EUR map of a production level at a gas interval of Mesaverde. There are two high productive portions with 2.5-3.5 BCF EUR wells. Note the consistency between high intensity anisotropy anomalies and portion (A). High permeable area with high fracture porosity support can explain this high produce portion (A).

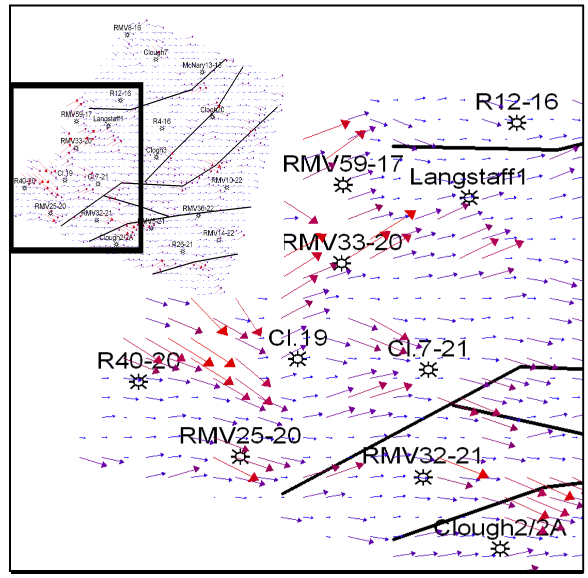

Figure 6: Anisotropy maps of a gas producer interval in Mesaverde. The westsouthern flank zoomed to demonstrate relationship between the best producer wells (EUR map) and the directional anisotropy. Note negative and positive focal points around CL-19 and CL-7-21 wells with more than 3.2 BCF EUR.

Conclusions

P-wave data from a wide azimuth 3D survey have been analyzed for anisotropy detection. In this regard a new robust processing sequence is designed to preserve anisotropy followed by a new interpretation technique to separate seismic anisotropy from the static and isotropic `geological' response. Faults and incoherent areas are interpreted using coherency attributes and 3D seismic amplitude cubes. There are reasonable correlation between faults patterns, incoherent anomalies and seismic anisotropy anomalies. Thus the predicted anisotropy anomalies can be a useful indicator of the fracturing within each fault compartment.
In low matrix and low permeability fractured reservoirs, the greater the EUR (expected ultimate recovery), the greater the fracture density. The results also show the anisotropy anomalies are propotional to EUR for the interval of the gas saturated Mesaverde.
Such information is important to include in the reservoir model for accurate simulation and its consequent predictions.

Acknowledgments

We acknowledge Shell for providing a Ph.D studentship. We would also like to thank Heloise Lynn (Lynn Inc.) and Rich Van Dok (Western-Geco) Doug Ostby (Williams Production RMT Co) for providing the original data.

References

Brown, R., Parra, J. and Xu, P., 2001, Seismic attenuation and flow properties in fractured reservoirs, 71st Ann. Internat. Mtg: Soc. of Expl. Geophys., 1678-1681.

Lynn, H. B., Campagna, D., Simon, K. M. and Beckham, W. E., 1999, Relationship of P-wave seismic attributes, azimuthal anisotropy, and commercial gas pay in 3-D P-wave multiazimuth data, Rulison Field, Piceance Basin, Colorado: GEOPHYSICS, Soc. of Expl. Geophys, 64, 1293-1311.

MacBeth, C., and Pickup, G., 2002. Estimation of directional permeability in fractured reservoirs – concepts and applications, Ann. Internat. Mtg, Soc.Explor. Geophys.,Salt Lake City.

MacBeth, C., 2002. Multi component VSP analysis for applied seismic anisotropy, Handbook of Exploration Geophysics, Volume 26, Pergamon.

Shams, A., and MacBeth, C., 2002. Robust time-lapse *AVOA* analysis using *OBC*: a case study from Teal South, Gulf of Mexico, 72nd Ann. Internat. Mtg. Soc. Expl. Geophys, Salt Lake City

Shams, A. and MacBeth, C., 2003, Detection of Saturation Changes in a Turbidite Sand by 4D AVOA, 65th Mtg.: Eur. Assn. Geosci. Eng., session: Reservoir monitoring.